A Simple Method to Realize Millilens Array on Encapsulant Layer for Enhancing Light Efficiency of COB-LEDs

Xingjian Yu, Linyi Xiang, Naiqi Pei, Shuling Zhou, and Xiaobing Luo, *Fellow, IEEE*

***Abstract*— The chip-on-board light-emitting diodes (COB-LEDs) present low light efficiency due to the total internal reflection (TIR) at the flat encapsulant–air interface. In this study, a simple method based on complementary printing was proposed to realize the millilens array on the flat encapsulant layer to diminish the TIR effect, and thereby improve the light efficiency of the COB-LEDs. Experiments and optical simulation based on the Monte Carlo ray-tracing method were conducted to investigate the effect of the lens curvature θ, lens radius *R*, and lens spacing *D* on the light efficiency of the COB-LEDs. The results show that the light efficiency of the COB-LEDs increases with *R* and decreases with *D*, and COB-LEDs with hemispherical lens arrays ($\theta = 90°$) have the highest light efficiency when *R* and *D* are fixed. Compared with the conventional COB-LEDs with a flat encapsulant, closely arranged hemispherical lens arrays with an *R* of 0.5, 1, and 1.5 mm enhance the light efficiency of the blue COB-LEDs by 87.56%, 90.62%, and 95.73% and enhance the light efficiency of ~6000-K white COB-LEDs by 17.24%, 18.86%, and 20.33%, respectively.**

***Index Terms*— Chip-on-board light-emitting diodes (COB-LEDs), light efficiency, millilens array, total internal reflection (TIR).**

I. Introduction

NOWADAYS, white light-emitting diodes (LEDs) are the mainstream lighting source due to its outstanding performance of high light efficiency, long lifetime, and compact size [1]. In LED packaging, the phosphor/silicone encapsulant layer is necessary for light conversion, color mixing, and oxygen/moisture protection [2]–[4]. As shown in Fig. 1, due to the refractive index difference of the LED chip (~2.5), encapsulant (1.4~1.7), and air (=1), serious total internal reflection (TIR) happens at the chip–encapsulant and encapsulant–air interfaces with the critical incident angles of $\theta_{\text{chip}-\text{encap}} < 43°$ and $\theta_{\text{encap}-\text{air}} < 46°$, which induces a significant light efficiency drop.

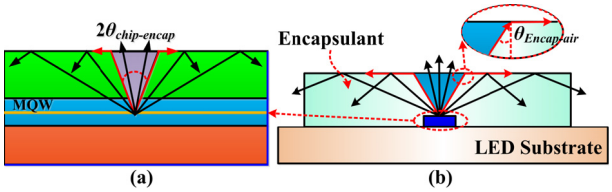

Fig. 1. TIR phenomenon at (a) chip–encapsulant interface and (b) encapsulant–air interface.

To diminish the TIR phenomenon at the chip–encapsulant interface, microlens arrays with spherical cap [5]–[11], spherical [12]–[15], cone [16], and domed [17] geometries were fabricated on the LED chips by photolithography [5]–[8] and nanomicrosphere deposition [13], [14]. The results show that the light-extraction efficiency of the LED chips can be improved by 20% to 4.5 times depending on the lens radius, curvature, and spacing of the lens array. In addition, the lens array with a hemispherical geometry was confirmed to have better optical performance than most of the other geometries.

Compared with the chip–encapsulant interface, the TIR phenomenon at the encapsulant–air interface did not receive extensive attention in the past decades, because the single-chip LEDs with an overall lens shown in Fig. 2(a) are the mainstream commercial LEDs. The overall lens guides the light to emit out from the encapsulant–air interface directly, and therefore improves the light efficiency of the LEDs. However, with the increasing packaging requirement of high power and compact size, chip-on-board LEDs (COB-LEDs) with dozens to hundreds of LED chips mounted on a large area flat substrate shown in Fig. 2(b) are becoming more and more popular. The substrate area of the COB-LEDs is dozens to hundreds of times of that of the single-chip LEDs. Therefore, it is impossible to use the overall lens to diminish the TIR, because it consumes too much silicone to fill the lens-encapsulant gap and increases the module's size significantly. As a result, the commercial COB-LEDs present a flat encapsulant–air interface shown in Fig. 2(b), which induces serious TIR at the encapsulant–air interface and decreases the light efficiency significantly.

Manuscript received June 13, 2020; revised July 4, 2020; accepted July 7, 2020. Date of publication July 27, 2020; date of current version August 21, 2020. This work was supported in part by the National Natural Science Foundation of China under Grant 51625601, in part by the Ministry of Science and Technology of the People's Republic of China under Grant 2017YFE0100600, in part by the Creative Research Groups Funding of Hubei Province under Grant 2018CFA001, in part by the Open Project Program of Wuhan National Laboratory for Optoelectronics under Grant 2018WNLOKF017, and in part by the Postdoctoral Creative Research Funding of Hubei Province. The review of this article was arranged by Editor C. Bayram. *(Corresponding author: Xiaobing Luo.)*

The authors are with the School of Energy and Power Engineering, Huazhong University of Science and Technology, Wuhan 430074, China (e-mail: luoxb@hust.edu.cn).

Color versions of one or more of the figures in this article are available online at http://ieeexplore.ieee.org.

Digital Object Identifier 10.1109/TED.2020.3008371

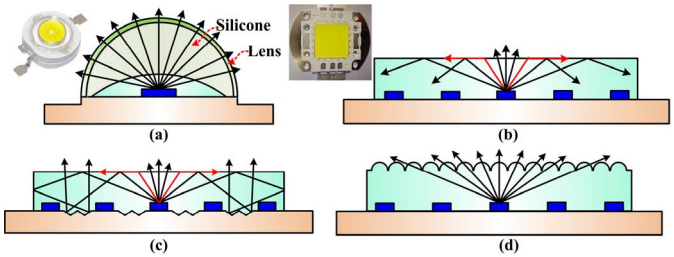

Fig. 2. Schematic of light propagation in (a) single-chip LEDs with overall hemispherical lens, (b) COB-LEDs without lens, (c) COB-LEDs with the patterned substrate, and (d) COB-LEDs with the dome-shaped encapsulant layer.

Few methods were proposed to diminish the TIR at the encapsulant–air interface of the COB-LEDs, including patterned substrate [18], scattering materials [19], and dome-shaped encapsulant layer [20]–[22]. The patterned substrate shown in Fig. 2(c) and the scattering materials redirect the reflected light to the critical angle, while the dome-shaped encapsulant layer shown in Fig. 2(d) guides the light to emit out from the encapsulant–air interface directly, which was proved to have higher light efficiency enhancement (LEE) than other methods [20]–[22]. Compared with the reported dome-shaped encapsulant layers, the encapsulant layer with an optimized lens array is expected to improve further the light efficiency of the COB-LEDs. However, the encapsulant layer is made of flexible resin, so the photolithography and nanomicrosphere-deposition methods are not suitable for realizing the lens array on the encapsulant layer due to the complicated wetting and curing behaviors of the encapsulant [23]. Instead, printing was confirmed to be an effective method to realize the texture structure on the encapsulant, because the mold regulates the wetting and curing behaviors of the encapsulant [24]. However, it is expensive to make molds with subtle and complex texture.

In this study, a simple method based on complementary printing was proposed to fabricate the millilens array on the flat encapsulant layer for improving the light efficiency of the COB-LEDs with 100 LED chips in a 10×10 array. First, the influence of lens curvature, radius, and spacing on the light efficiency of the COB-LEDs was investigated by the Monte Carlo ray-tracing method. Then, the lens arrays with various lens radii and curvature were fabricated on the encapsulant layer by the proposed method and the light efficiency of the COB-LEDs with lens arrays was measured and analyzed.

II. Methodology

A. Experiment

Fig. 3 shows the fabricating process of the millilens array, and it consists of the following steps.

1) Coating a thin binder (Deli, 7148AB) layer on a flat substrate with a coating machine (Weida, AFA-V) and depositing steel balls on the binder layer.
2) Printing ethylene-vinyl acetate (EVA) resin on the steel ball array with a hot melt glue gun (Deli, DL5041) and removing the EVA resin after 10 min. Due to the existence of the steel balls, the EVA resin has concave spherical cap pits on one side, which could be used as mold for making the lens array.
3) Coating silicone (Dow Corning, DC-184) on a flat surface, putting the EVA mold on the silicone layer, and heating the silicone to 55 °C for 60 min to cure it. Removing the EVA mold and silicone film with a lens array is obtained.

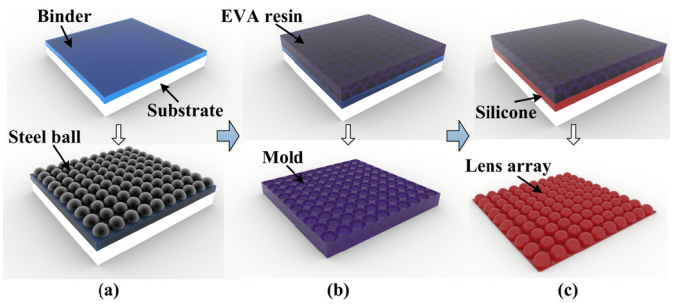

Fig. 3. Fabrication process of the milli-lens array. (a) Fabrication of steel ball array. (b) Fabrication of EVA mold. (c) Realization of millilens array.

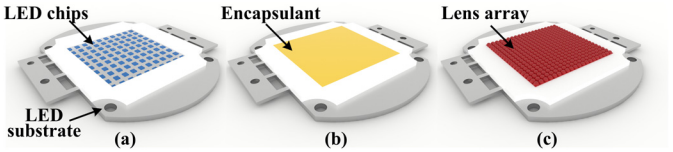

Fig. 4. Schematic of the COB-LEDs used in this study. (a) Without encapsulant. (b) With phosphor/silicone encapsulant. (c) With lens array.

In this process, the geometry of the steel ball array, EVA mold, and lens array is complementary, so the geometry of the lens array is the same as that of the steel ball array. The geometry of the steel ball array is determined by the thickness of the binder, the radius, and the arrangement of the steel balls. Therefore, lens arrays with various lens curvatures, radii, and spacings can be realized by manipulating the thickness of the binder, the radius, and the arrangement of the steel balls.

Fig. 4(a) shows the COB-LED module used in this study. Hundred conventional chips with a size of 1 mm × 1 mm are mounted on a flat substrate of 20 mm × 20 mm in a 10 × 10 array. After coating phosphor/silicone encapsulant on the LED chips shown as Fig. 4(b), attach the lens array on the encapsulant shown as Fig. 4(c) and heat the encapsulant to 100 °C for 30 min to cure the encapsulant.

In the experiments, blue and ∼6000-K white COB-LEDs without and with lens arrays were fabricated. For the blue COB-LEDs, silicone (Dow Corning, DC-184) with a refractive index of ∼1.41 was used as the encapsulant. For the white COB-LEDs, the silicone/phosphor (YAG-O4, Intematix) mixture with a mass concentration of 0.03:1 g was used as the encapsulant. The thickness of the encapsulant layer was set as ∼1 mm. The light efficiency of the COB-LEDs with and without lens arrays was measured by an integrating sphere (ATA-1000, Everfine). During the optical measurement, the COB-LED modules were placed on a cold plate with a constant temperature of 25 °C to keep them cooled.

B. Optical Simulation

The effect of lens curvature θ, lens radius R, and lens spacing D shown in Fig. 5(b) on the light efficiency of the

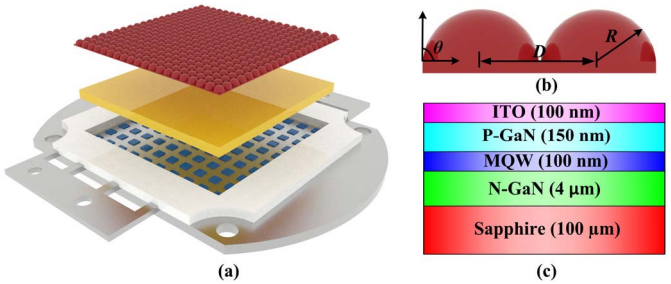

Fig. 5. Optical simulation. (a) Simulation model. (b) Schematic of the lens curvature θ, radius R, and spacing D. (c) Structure of the conventional chip.

TABLE I
OPTICAL PROPERTIES OF THE CHIP LAYERS

Layers	Wavelength	454 nm	570 nm
Sapphire	Refractive Index	1.77	1.77
	Absorption Coefficient (mm^{-1})	0	0
N-GaN	Refractive Index	2.43	2.36
	Absorption Coefficient (mm^{-1})	2	1.5
MQW	Refractive Index	2.51	2.39
	Absorption Coefficient (mm^{-1})	8	8
P-GaN	Refractive Index	2.43	2.36
	Absorption Coefficient (mm^{-1})	2	1.5
ITO	Refractive Index	2	1.9
	Absorption Coefficient (mm^{-1})	0	0

COB-LEDs was investigated by the Monte Carlo ray-tracing method. Fig. 5(a) shows the simulation model. The structure of the COB-LED is the same as the experimental COB-LED, including the chip size, distribution, and thickness of the encapsulant. The structure of the conventional chip is shown in Fig. 3(b), and the optical properties of the chip layers are shown in Table I [22]. The input optical power of each chip was set as 1 W. The refractive index of the silicone was set as 1.41. The reflectance and absorptance of the LED substrate were set as 0.92 and 0.08, respectively. For the white COB-LEDs, the phosphor was assumed to be spherical with a diameter of 13-μm, and its mass concentration with the silicone was set as 0.03:1 g. To simulate the light-conversion process, specific wavelengths of 454 and 570 nm were used to characterize the emission light of the LED chips and phosphor. In the simulations, θ varies from 0° to 120°, R varies from 0.25 to 1.5 mm, and D varies from 1 to 3 mm.

III. RESULTS AND DISCUSSION

Fig. 6 shows the simulated LEE of the blue and ~6000-K white COB-LEDs by a lens array with various values of θ, R, and D. The LEE is defined as $(\eta_{\text{lens}} - \eta_{\text{flat}})/\eta_{\text{flat}} \times 100\%$, where η_{flat} is the light efficiency of the COB-LEDs with a flat encapsulant layer and η_{lens} is the light efficiency of the COB-LEDs with a lens array. Fig. 6(a) shows that the LEE of the COB-LEDs increases with θ when $\theta < 90°$ and decreases with θ afterward, when R and D are fixed as 0.5 and 1 mm. If θ is smaller or larger than 90°, the light at the side emitting angle would be reflected, as shown in the inset of Fig. 6(a), which decreases the light efficiency of the COB-LEDs. Therefore, θ of 90° (lens with hemispherical geometry) is optimal [20]–[22]. Fig. 6(b) shows that the LEE

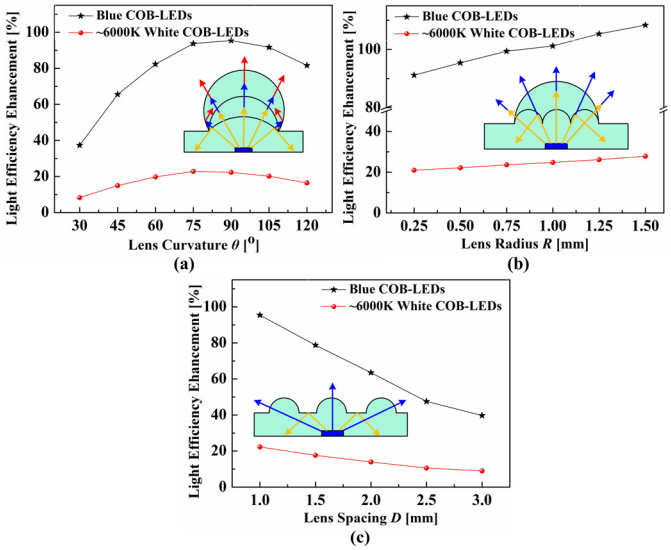

Fig. 6. Simulated LEE of the blue and ~6000-K white COB-LEDs by lens arrays with various (a) lens curvatures, (b) lens radii, and (c) lens spacings.

of the COB-LEDs increases with R, when θ and D are fixed as 90° and $2R$. Larger R means the LED chip is closer to the point light source, so more light emits out from the encapsulant–air interface directly, as shown in the inset of Fig. 6(b). Fig. 6(c) shows that the LEE of the COB-LEDs decreases with D, when θ and R are fixed as 90° and 0.5 mm. The area proportion of the flat surface to the entire surface increases with D, so more light would be reflected, as shown in the inset of Fig. 6(c). As a result, the light efficiency of the COB-LEDs decreases.

The above results indicate that the lens array enhances the light efficiency of the COB-LEDs significantly. Moreover, it shows that the LEE of the white COB-LEDs is smaller than that of the blue COB-LEDs. This is caused by the scattering effect of phosphors [19], [22]. As shown in the inset of Fig. 7(b), the phosphors redirect part of the light to the critical angle, which increases the light efficiency of the COB-LEDs. As a result, the LEE of the white COB-LEDs by the lens arrays is weakened.

Fig. 7 shows the simulated blue and yellow light radiant powers of the white COB-LEDs with various lens arrays. The blue and yellow light powers follow the same change rule with the lens curvature, radius, and spacing. In addition, Fig. 7(a) shows that the radiant power of the blue COB-LEDs with a flat encapsulant is 11.16 W, while the radiant power of ~6000-K white COB-LEDs with a flat encapsulant is 15.98 W (sum of the blue and yellow light radiant powers), which proves that the scattering effect of phosphor increases the light efficiency of the COB-LEDs.

The simulated results show that lens arrays with $\theta = 90°$ and $D = 2R$ have the highest light efficiency. In the experiments, it is hard to control the lens spacing, because the steel balls are deposited on the binder layer randomly. Therefore, D was controlled as $\sim 2R$ by depositing the steel balls closely. Moreover, lens arrays with various values of θ and R were obtained by changing the thickness of the binder and the radius of the steel balls.

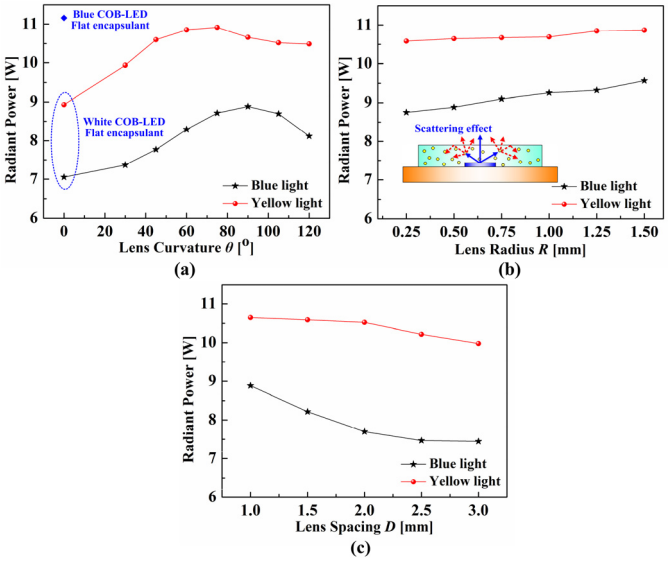

Fig. 7. Simulated blue and yellow light radiant powers of the white COB-LEDs with various (a) lens curvatures, (b) lens radii, and (c) lens spacings.

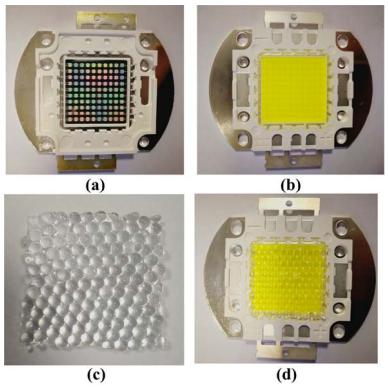

Fig. 8. Photographs of (a) blue COB-LEDs with a flat silicone encapsulant, (b) ~6000-K white COB-LEDs with a flat phosphor/silicone encapsulant, (c) lens array with $R = 1$ mm, $\theta = \sim 90°$, and $D = \sim 2$ mm, and (d) white COB-LEDs with lens array.

Fig. 8(a) and (b) shows the blue and white COB-LEDs with a flat encapsulant layer used in the experiments. Fig. 8(c) shows the lens array with $R = 1$ mm, $\theta = \sim 90°$, and $D = \sim 2$ mm, and Fig. 8(d) shows the white COB-LEDs with the lens array shown in Fig. 8(c).

Fig. 9 shows the photographs of the lens arrays with $R = 1.5$ mm, $D = \sim 3$ mm, and $\theta = \sim 30°$, $\sim 60°$, and $\sim 90°$. It is very difficult to realize the lens array with $\theta > 90°$ due to the difficulties in the EVA mold and lens array removing processes. Fig. 10(a) shows the light efficiency of blue and ~6000-K white COB-LEDs with lens arrays shown in Fig. 9. Compared with the COB-LEDs with a flat encapsulant, the LEE of the COB-LEDs by the lens arrays is shown in Fig. 10(b). It shows that when θ is ~30°, ~60°, and ~90°, the LEEs of the blue COB-LEDs are 36.21%, 83.31%, and 95.73%, and the LEEs of the white COB-LEDs are 6.39%, 16.93%, and 20.33%.

Fig. 11 shows the photographs of the lens arrays with $D = \sim 2R$, $\theta = \sim 90°$, and $R = 0.5$, 1, and 1.5 mm. Fig. 12(a) shows the light efficiency of blue and ~6000-K white COB-LEDs with lens arrays shown in Fig. 11. Compared

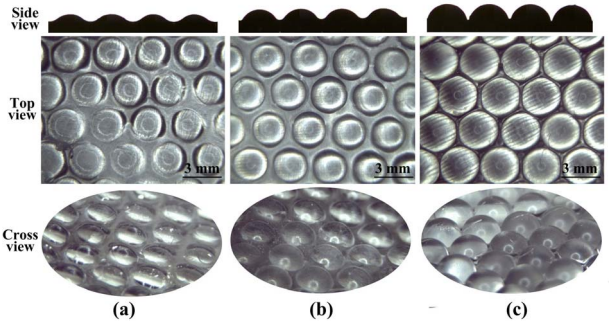

Fig. 9. Photographs of the lens arrays with $R = 1.5$ mm, $D = \sim 3$ mm, and $\theta =$ (a) ~30°, (b) ~60°, and (c) ~90°.

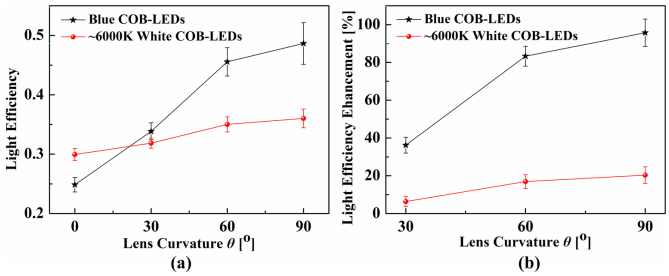

Fig. 10. (a) Light efficiency of the blue and ~6000-K white COB-LEDs without and with the lens arrays shown in Fig. 9. (b) LEE of the blue and ~6000-K white COB-LEDs by the lens arrays shown in Fig. 9.

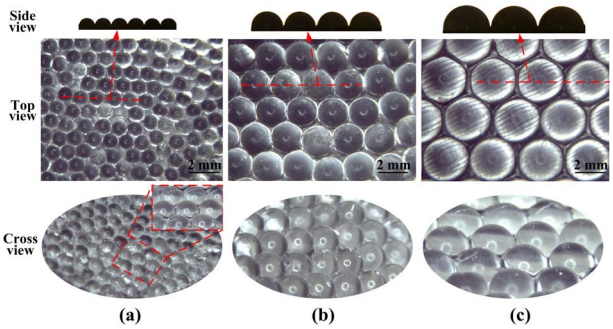

Fig. 11. Photograph of lens arrays with $D = \sim 2R$, $\theta = \sim 90°$, and $R =$ (a) 0.5, (b) 1, and (c) 1.5 mm.

with the COB-LEDs with a flat encapsulant, the LEE of the COB-LEDs by the lens arrays is shown in Fig. 12(b). It shows that when R is 0.5, 1, and 1.5 mm, the LEEs of the blue COB-LEDs are 87.56%, 90.62%, and 95.73%, and the LEEs of the white COB-LEDs are 17.24%, 18.86%, and 20.33%.

The experimental results show that the light efficiency of the COB-LEDs increases with θ and R, which is consistent with the simulated results. In addition, the deviation of the LEE obtained from simulations and the maximum LEE obtained from experiments is <10%. Although the light efficiency of the COB-LEDs increases with R, it is inadvisable to use large R, because it consumes too much silicone and increases the module's size.

Fig. 13 summarizes the LEE of the COB-LEDs by the lens array and previous methods, and the parameters of the lens array used for comparison are $R = 1.5$ mm, $D = \sim 3$ mm, and $\theta = \sim 90°$. It shows that the LEE of the COB-LEDs by the lens array is much higher than other methods, which indicates the superiority of the lens array.

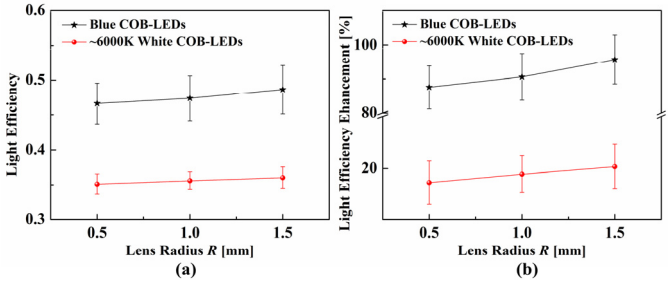

Fig. 12. (a) Light efficiency of the blue and ~6000-K white COB-LEDs with the lens arrays shown in Fig. 11. (b) LEE of the blue and ~6000-K white COB-LEDs by the lens arrays shown in Fig. 11.

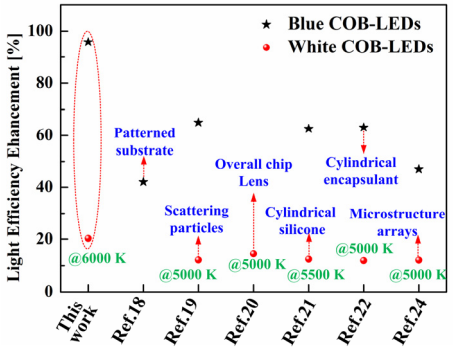

Fig. 13. Comparison of the LEE of the COB-LEDs by the lens array and previous works.

IV. Conclusion

In this study, a simple method based on complementary printing was proposed to realize the millilens array on the encapsulant layer for enhancing the light efficiency of the COB-LEDs. Optical simulations based on the Monte Carlo ray-tracing method were applied to investigate the influence of lens curvature θ, lens radius R, and lens spacing D on the light efficiency of the COB-LEDs. Experiments were conducted to fabricate the lens arrays with various values of θ and R. The results show that the light efficiency of the COB-LEDs increases with R and decreases with D, and the COB-LEDs with hemispherical lens arrays ($\theta = 90°$) have the highest light efficiency. The experimental results show that compared with the conventional COB-LEDs with a flat encapsulant, the LEEs of blue and ~6000-K white COB-LEDs by the lens array with $D = \sim 3$ mm, $\theta = \sim 90°$, and $R = 1.5$ mm are 95.73% and 20.33%, which is much higher than that reported in the previous studies. This study is helpful for promoting the future application of the lens array in the COB-LED packaging.

References

[1] X. Luo, R. Hu, S. Liu, and K. Wang, "Heat and fluid flow in high-power LED packaging and applications," *Prog. Energy Combustion Sci.*, vol. 56, pp. 1–32, Sep. 2016, doi: 10.1016/j.pecs.2016.05.003.

[2] Y. Peng *et al.*, "Flexible fabrication of a patterned red phosphor layer on a YAG:Ce^{3+} phosphor-in-glass for high-power WLEDs," *Opt. Mater. Exp.*, vol. 8, no. 3, pp. 605–614, 2018, doi: 10.1364/OME.8.000605.

[3] X. Yu, B. Xie, Q. Chen, Y. Ma, R. Wu, and X. Luo, "Thermal remote phosphor coating for phosphor-converted white-light-emitting diodes," *IEEE Trans. Compon., Packag., Manuf. Technol.*, vol. 5, no. 9, pp. 1253–1257, Sep. 2015, doi: 10.1109/TCPMT.2015.2453397.

[4] Y. Peng, Y. Mou, Q. Sun, H. Cheng, M. Chen, and X. Luo, "Facile fabrication of heat-conducting phosphor-in-glass with dual-sapphire plates for laser-driven white lighting," *J. Alloys Compounds*, vol. 790, pp. 744–749, Jun. 2019, doi: 10.1016/j.jallcom.2019.03.220.

[5] D. Kim, H. Lee, N. Cho, Y. Sung, and G. Yeom, "Effect of GaN microlens array on efficiency of GaN-based blue-light-emitting diodes," *Jpn. J. Appl. Phys.*, vol. 44, nos. 1–7, pp. 42–45, 2005, doi: 10.1143/JJAP.44.L18.

[6] H. W. Choi *et al.*, "GaN micro-light-emitting diode arrays with monolithically integrated sapphire microlenses," *Appl. Phys. Lett.*, vol. 84, no. 13, pp. 2253–2255, Mar. 2004, doi: 10.1063/1.1690876.

[7] M. Khizar, Z. Y. Fan, K. H. Kim, J. Y. Lin, and H. X. Jiang, "Nitride deep-ultraviolet light-emitting diodes with microlens array," *Appl. Phys. Lett.*, vol. 86, no. 17, pp. 1–3, 2005, doi: 10.1063/1.1914960.

[8] R. Liang *et al.*, "High light extraction efficiency of deep ultraviolet LEDs enhanced using nanolens arrays," *IEEE Trans. Electron Devices*, vol. 65, no. 6, pp. 2498–2503, Jun. 2018, doi: 10.1109/TED.2018.2823742.

[9] Y. Qu, J. Kim, C. Coburn, and S. R. Forrest, "Efficient, nonintrusive outcoupling in organic light emitting devices using embedded microlens arrays," *ACS Photon.*, vol. 5, no. 6, pp. 2453–2458, Jun. 2018, doi: 10.1021/acsphotonics.8b00255.

[10] F. Galeotti, W. Mróz, G. Scavia, and C. Botta, "Microlens arrays for light extraction enhancement in organic light-emitting diodes: A facile approach," *Organic Electron.*, vol. 14, no. 1, pp. 212–218, Jan. 2013, doi: 10.1016/j.orgel.2012.10.034.

[11] E. Wrzesniewski *et al.*, "Enhancing light extraction in top-emitting organic light-emitting devices using molded transparent polymer microlens arrays," *Small*, vol. 8, no. 17, pp. 2647–2651, Sep. 2012, doi: 10.1002/smll.201102662.

[12] X. Chen, K. Li, F. Kong, J. Wang, and L. Zhang, "Improved the light extraction efficiency of GaN vertical light-emitting diodes using 3D sphere-like arrays," *Opt. Quantum Electron.*, vol. 47, no. 8, pp. 2957–2968, Aug. 2015, doi: 10.1007/s11082-015-0181-7.

[13] Z. Zhu *et al.*, "Improvement of light extraction of LYSO scintillator by using a combination of self-assembly of nanospheres and atomic layer deposition," *Opt. Express*, vol. 23, no. 6, p. 7085, 2015, doi: 10.1364/oe.23.007085.

[14] J. Y. Park, G. S. Rama Raju, B. K. Moon, and J. H. Jeong, "Facile solvothermal synthesis of high refractive index ZrO_2 spheres: Estimation of the enhanced light extraction efficiency," *RSC Adv.*, vol. 5, no. 100, pp. 81915–81919, 2015, doi: 10.1039/c5ra13284c.

[15] Z. C. Zhu, B. Liu, C. Cheng, Y. Yi, H. Chen, and M. Gu, "Improved light extraction efficiency of cerium-doped lutetium-yttrium oxyorthosilicate scintillator by monolayers of periodic arrays of polystyrene spheres," *Appl. Phys. Lett.*, vol. 102, no. 7, pp. 1–4, 2013, doi: 10.1063/1.4793303.

[16] P. Zhu, H. Zhu, S. Thapa, and G. C. Adhikari, "Design rules for white light emitters with high light extraction efficiency," *Opt. Express*, vol. 27, no. 16, Aug. 2019, Art. no. A1297, doi: 10.1364/oe.27.0a1297.

[17] P. Zhao and H. Zhao, "Analysis of light extraction efficiency enhancement for thin-film-flip-chip InGaN quantum wells light-emitting diodes with GaN micro-domes," *Opt. Express*, vol. 20, no. S5, p. A765, Sep. 2012, doi: 10.1364/OE.20.00A765.

[18] Z.-T. Li, Q.-H. Wang, Y. Tang, C. Li, X.-R. Ding, and Z.-H. He, "Light extraction improvement for LED COB devices by introducing a patterned leadframe substrate configuration," *IEEE Trans. Electron Devices*, vol. 60, no. 4, pp. 1397–1403, Apr. 2013, doi: 10.1109/TED.2013.2248063.

[19] H. Zheng, L. Li, X. Lei, X. Yu, S. Liu, and X. Luo, "Optical performance enhancement for chip-on-board packaging LEDs by adding TiO2/Silicone encapsulation layer," *IEEE Electron Device Lett.*, vol. 35, no. 10, pp. 1046–1048, Oct. 2014, doi: 10.1109/LED.2014.2349951.

[20] X. Yu, B. Xie, B. Shang, W. Shu, and X. Luo, "A facile approach to fabricate patterned surfaces for enhancing light efficiency of COB-LEDs," *IEEE Trans. Electron Devices*, vol. 64, no. 10, pp. 4149–4155, Oct. 2017, doi: 10.1109/TED.2017.2734105.

[21] X. Yu, R. Hu, R. Wu, B. Xie, X. Zhang, and X. Luo, "Cylindrical tuber encapsulant layer realization by patterned surface for chip-on-board light-emitting diodes packaging," *J. Electron. Packag.*, vol. 141, no. 3, pp. 1–5, Sep. 2019, doi: 10.1115/1.4042982.

[22] X. Yu, B. Xie, B. Shang, Q. Chen, and X. Luo, "A cylindrical tuber encapsulant geometry for enhancing optical performance of chip-on-board packaging light-emitting diodes," *IEEE Photon. J.*, vol. 8, no. 3, pp. 1–9, Jun. 2016, doi: 10.1109/JPHOT.2016.2555619.

[23] X. J. Yu, R. Hu, L. L. Zhou, H. Wu, and X. B. Luo, "Spreading and curing behaviors of a thermosetting droplet-silicone on a heated surface," *J. Harbin Insitute Technol.*, vol. 26, no. 4, pp. 1–8, 2019.

[24] D. Wu, K. Wang, and S. Liu, "Enhancement of light extraction efficiency of multi-chips light-emitting diode array packaging with various microstructure arrays," in *Proc. IEEE 61st Electron. Compon. Technol. Conf.*, May/Jun. 2011, pp. 242–245, doi: 10.1109/ECTC.2011.5898520.